Published in final edited form as:
Gastroenterology. 2007 August ; 133(2): 619–631. doi:10.1053/j.gastro.2007.05.018.

Granulocyte–Colony Stimulating Factor Promotes Liver Repair and Induces Oval Cell Migration and Proliferation in Rats

ANNA C. PISCAGLIA[*,‡], **THOMAS D. SHUPE**[*], **SEH–HOON OH**[*], **ANTONIO GASBARRINI**[‡], and **BRYON E. PETERSEN**[*,§]

[*] Department of Pathology, Immunology and Laboratory Medicine, College of Medicine, University of Florida, Gainesville, Florida

[‡] Department of Internal Medicine and Gastroenterology, Catholic University of Rome, Rome, Italy

[§] the Program for Stem Cell Biology, University of Florida—Shands Cancer Center, Gainesville, Florida

Abstract

Background & Aims—Hepatic regeneration is a heterogeneous phenomenon involving several cell populations. Oval cells are considered liver stem cells, a portion of which derive from bone marrow (BM). Recent studies have shown that granulocyte–colony stimulating factor (G-CSF) may be effective in facilitating liver repair. However, it remains unclear if G-CSF acts by mobilizing BM cells, or if it acts locally within the liver microenvironment to facilitate the endogenous restoration program. In the present study, we assessed the involvement of G-CSF during oval cell activation.

Methods—Dipeptidyl-peptidase-IV–deficient female rats received BM transplants from wild-type male donors. Four weeks later, rats were subjected to the 2-acetylaminofluorene/partial hepatectomy model of oval cell–mediated liver regeneration, followed by administration of either nonpegylated G-CSF or pegylated G-CSF. Control animals did not receive further treatments after surgery. The magnitude of oval cell reaction, the entity of BM contribution to liver repopulation, as well as the G-CSF/G-CSF–receptor expression levels were evaluated. In addition, in vitro proliferation and migration assays were performed on freshly isolated oval cells.

Results—Oval cells were found to express G-CSF receptor and G-CSF was produced within the regenerating liver. G-CSF administration significantly increased both the magnitude of the oval cell reaction, and the contribution of BM to liver repair. Finally, G-CSF acted as a chemoattractant and a mitogen for oval cells in vitro.

Conclusions—We have shown that G-CSF facilitates hepatic regeneration by increasing the migration of BM-derived progenitors to the liver, as well as enhancing the endogenous oval cell reaction.

Liver regeneration is a heterogeneous phenomenon, involving at least 3 levels of proliferating cells: mature hepatocytes, ductular progenitors, and oval cells.[1] The term *oval cells* (OCs) defines small proliferating cells with an oval-shaped nucleus and a high nuclear to cytoplasm ratio, which appear within the liver after certain models of injury and carcinogenesis.[2] OCs are bipotential, sharing the ability to differentiate into hepatocytes and

Address requests for reprints to: Anna C. Piscaglia, MD, Department of Pathology, 1600 SW Archer Road, MSB—Room M641, University of Florida, College of Medicine, Gainesville, Florida 32610. piscag@pathology.ufl.edu or annachiarapiscaglia@hotmail.com; fax: (352) 392-6249.

biliary epithelial cells, and, therefore, represent putative liver stem cells.[2] In OC-mediated liver regeneration, OCs arise from the portal tract periphery and migrate into the lobular parenchyma. Trafficking, mobilization, and homing of OCs are regulated by several factors, including adhesion molecules, cytokines, and chemotactic molecules.[3] As for their origin, some believe that OCs derive from ductular cells of the canals of Hering, whereas others speculate that they arise from liver-committed circulating stem cells of extrahepatic origin.[4] Numerous studies conducted on animal models and human beings have suggested that bone marrow cells (BMCs) may give rise to OCs.[5–9] In vitro studies also have shown that a subpopulation of BMCs expresses hepatic markers and, conversely, that OCs express hematopoietic antigens such as CD34, c-kit, and Thy-1.[10,11]

Mobilization of BMCs into the circulation can be induced by a wide variety of molecules such as cytoreductive drugs, chemokines, and hematopoietic cytokines.[12] Granulocyte–colony stimulating factor (G-CSF) is among the most commonly used BMC mobilizing agents because of its potency and lack of toxicity.[13] The biological effects of G-CSF are mediated predominantly through the G-CSF receptor (G-CSFR), and partly through *trans*-activating signals within the BM microenvironment.[14] Recent studies have suggested that G-CSF may be effective in mobilizing cells that contribute to liver repair after damage.[15–18] However, it remains unclear if G-CSF acts mainly by recruiting BMCs, or if it acts locally within the liver microenvironment to facilitate the endogenous hepatic restoration program. The potential trophic effects of G-CSF on liver stem cells could have a dramatic clinical impact because G-CSF is one of the few growth factors approved for use in patients.[13]

In the present study, we sought to assess the role of G-CSF during OC-mediated liver regeneration. We used the well-established model of OC activation in rats, involving the administration of 2-acetylaminofluorene (2AAF) before partial hepatectomy (PH).[19] 2AAF is metabolized selectively by hepatocytes to an N-hydroxyl derivative, which interferes with the cyclin-D_1 pathway. Therefore, the administration of 2AAF before PH inhibits hepatocyte proliferation and forces OC recruitment to mediate liver regeneration. This procedure results in a robust OC response after PH (peaking between days 9 and 11), and within 14 days OCs begin to differentiate into hepatocytes.[20] In addition, we have investigated the effects of G-CSF administration after 2AAF/PH in terms of magnitude of the OC response, as well as the degree of BMC contribution to the regenerative process. To assess the BM contribution to liver repopulation, we used the dipeptidyl-peptidase-IV (DPPIV)-deficient rat model.[5] DPPIV is an exopeptidase expressed by many cell types, including BM, blood, and hepatic cells. After BM transplantation (BMTx) from wild-type rats into $DPPIV^-$ animals, the expression of DPPIV can be used to detect donor-derived cells in the chimeric recipients. Finally, we have evaluated the effects of G-CSF on OCs through in vitro assays. We have shown that G-CSF enhances hepatic regeneration after BMTx/2AAF/PH in rats by mobilizing liver committed BMCs, as well as by promoting migration and proliferation of endogenous OCs.

Materials and Methods

Animal Treatments

Animals—$DPPIV^-$ F344 female rats (age, 8 –10 wk) were in-house bred and maintained on standard laboratory chow and daily cycles, alternating 12 hours of light and dark. Wild-type F344 male rats (age, 8 –10 wk) were purchased from Charles River Laboratories (Wilmington, MA). All procedures were performed with the approval of the University of Florida Institutional Animal Care and Usage Committee. The experimental design is summarized in Figure 1.

BMC isolation and transplantation—Before BMTx, DPPIV^{-} female rats were exposed to total body γ-irradiation (^{137}Cs, JL Shepherd Mark-I; J.L. Shepherd and Associates, San Fernando, CA), administered in 2 doses of 450 rads each, 3 hours apart. BMCs were isolated from the long bones of donor rats. Cells were passed through a 130-μm cell strainer, collected by centrifugation at 220 × *g*, and resuspended in Iscove's modified Dulbecco's medium (IMDM) (GIBCO, Grand Island, NY). BMCs were transplanted into recipient rats via tail vein injection after irradiation (5×10^7 cells/rat). Three weeks later, the donor contribution to BM reconstitution was assessed through analysis of the presence of Y-chromosome and DPPIV in blood cells.

OC activation model and G-CSF administration—Recombinant methionyl human G-CSF (Filgrastim) and its pegylated counterpart (peg-Filgrastim, Peg–G-CSF) were kindly provided by Amgen Inc. (Thousand Oaks, CA). The 2AAF/PH regimen for OC induction was performed as previously described.[19] Briefly, 4 weeks after BMTx, chimeric animals were implanted intraperitoneally with a time-released 2AAF pellet (70 mg/28-day release; Innovative Research of America, Sarasota, FL). Seven days later, rats underwent PH, as described elsewhere.[21] Animals then were administered subcutaneously Peg–G-CSF (10 mg/kg in a single dose; group A), or nonpegylated G-CSF (250 μg/kg/day for 5 days; group B). Control rats did not receive any treatment after 2AAF/PH (group C). Postsurgery, animals were placed in general housing until death at 1, 3, 5, 7, 11, 15, and 28 days after PH (21 animals in each group, 3 rats/time point). Samples of liver tissue were collected separately in optical cut temperature embedding medium (Sakura Finetek USA, Inc, Torrance, CA), snapfrozen in liquid nitrogen, and embedded in paraffin after overnight fixation in 10% formalin.

Histology, Immunohistochemistry, and Immunofluorescence

For morphology studies, 5-μm paraffin sections were stained with H&E. Immunohistochemistry and immunofluorescence were performed either on 5-μm paraffin-embedded or OCT frozen sections using standard staining protocols. Immunophenotyping of liver samples used 1:100 mouse anti-Ki67 (proliferation index; BD Biosciences Pharmingen, San Diego, CA); 1:100 mouse anti-OV6 (oval and ductular cell marker; a generous gift from Dr Sell, Albany, NY); 1:100 sheep anti–α-fetoprotein (anti-AFP) (OCs and progenitor cell marker; Nordic Immunological Lab., Tilburg, The Netherlands); 1:100 mouse anti-CD45 (common leukocyte antigen; BD Biosciences Pharmingen); 1:100 rabbit anti–G-CSFR and 1:100 goat anti–G-CSF (both from Santa Cruz Biotechnologies, Santa Cruz, CA). Negative controls and isotype controls (Vector Laboratories, Burlingame, CA) showed negligible autofluorescence and nonspecific binding of primary antibodies to cells/tissue. Vector ABC-kit (Vector Laboratories) and 3,3′-diaminobenzidine tetrahydrochloride (DAB) reagent (Dakocytomation, Carpinteria, CA) were used in the immunoperoxidase detection procedure. For immunofluorescence staining, Vectastain kit with DAPI, Texas-red, and fluorescein-conjugated secondary antibodies (Vector Laboratories) were used. The enzymatic DPPIV staining procedure was performed as previously described.[22] To confirm the epithelial nature of donor-derived cells within the liver, double immunofluorescence for OV6 and CD26 was performed, using 1:100 goat anti-CD26 (anti-DPPIV, Santa Cruz Biotechnologies). Quantification of Ki67, OV6, and DPPIV^{+} cells was obtained through the analysis of 5– 8 fields selected randomly from each specimen (objective magnification, 20×). The samples were photographed using an Olympus microscope and an Optronics digital camera (Olympus, Melville, NY). Selected slides also were analyzed by confocal microscopy (Spectra Confocal Microscope TCS-SP2-AOBS, equipped with Software V. 2.61; Leica Microsystems Inc., Bannockburn, IL).

DNA Polymerase Chain Reaction, Reverse-Transcription Polymerase Chain Reaction, and Western Blotting

To assess the donor contribution to BM reconstitution, DNA polymerase chain reaction (PCR) analysis for the sexual region of the Y chromosome was performed 3 weeks after BMTx on DNA extracted from blood cells, as previously described.[5] Reverse-transcription (RT)-PCR analysis for G-CSFR was performed on RNA isolated from normal liver, freshly isolated OCs, and cultured OCs by using the RNeasy kit (Qiagen, Valencia, CA). cDNA was synthesized from 5 μg of total RNA. RT-PCR was performed as described elsewhere.[5] The resulting RT-PCR products were analyzed on 1.5% agarose gels stained with ethidium bromide. For Western blot analysis, frozen liver samples were thawed and total proteins were extracted from homogenates in RIPA buffer, separated by 8% sodium dodecyl sulfate–polyacrylamide gel electrophoresis and transferred to polyvinylidene-difluoride membranes. Immunoblotting was performed using 1:500 anti–G-CSF, 1:500 anti–G-CSFR, and 1:5000 anti–β-actin (Abcam Inc., Cambridge, MA). Immunocomplexes were detected with horseradish-peroxidase–conjugated secondary antibodies (Santa Cruz Biotechnologies). Detection was performed using the ECL plus kit (Amersham Life Science, Piscataway, NJ).

In Vitro Assays

Cytospins and in vitro assays were performed on OCs isolated from rats subjected to 2AAF/PH, as described elsewhere.[10,23] Briefly, isolation was achieved by using a standard 2-step collagenase perfusion. Cells were centrifuged at 55 × *g* to separate the hepatocyte fraction from nonparenchymal cells, the latter were collected at 220 × *g*. Nonparenchymal cells were incubated with Thy-1–fluorescein isothiocyanate– conjugated antibody (BD Biosciences Pharmingen), followed by incubation with anti–fluorescein isothiocyanate microbeads. Thy-1^+ OCs subsequently were selected using immunomagnetic sorting (MACS; Miltenyi Biotec Inc., Auburn, CA). Cell viability was determined to be greater than 90% by Trypan-blue dye exclusion.

Cytospins—Cytocentrifugation was performed on collected Thy-1^+ cells at 41 × *g* (Cytospin-4; Thermo-Shandon, Cheshire, England). Cytospin preparations (10^5 cells/slide) were stained for Thy-1, OV6, CD45, G-CSFR, and G-CSF as described earlier. For in vitro proliferation and migration assays 3 different doses of G-CSF were tested: 10 ng/mL, 100 ng/mL, and 500 ng/mL. All assays were performed in triplicate to ensure statistical significance. Antibiotic-antimycotic solutions were added to each buffer.

Proliferation assay—Cells (2×10^5) were seeded in 6-well plates in IMDM supplemented with 10% fetal bovine serum, 1% insulin, and were incubated at 37°C, 5% CO_2, overnight. The next day, medium was removed and the cells were cultured in different buffers: IMDM with 0.5% bovine serum albumin (negative control), IMDM with 10% fetal bovine serum (positive control), and IMDM with 0.5% bovine serum albumin and various doses of G-CSF (experimental groups). Cell counts were performed on trypsinized cells immediately before the test (day 1), and every subsequent 48 hours.

Migration assay—Cell motility was assessed in transwells, as previously described.[23] Briefly, transwell culture dishes (Coring, Inc., Costar, NY) with 5-μm pore filters were precoated overnight with 0.006% rat-tail collagen. Cells (1×10^5) were suspended in migration buffer (IMDM, 10% fetal bovine serum, and 1% insulin), and allowed to attach overnight. Nonadherent cells were removed from the top of the transwell chambers and the transwells then were transferred to new wells containing various doses of G-CSF in migration buffer. Plates were incubated at 37°C, 5% CO_2, for either 4 or 6 hours. As controls, G-CSF either was excluded from the lower chamber (migration control) or added to both the lower and upper chambers (chemokinetic control). At the end of the assay, cells

that had migrated to the bottom of the transwell filter were fixed, stained, and counted. Data were normalized for each independent experiment with respect to the migration control, and expressed as the relative chemotactic index.

Statistical Analysis

Values presented are expressed as mean ± SD. After acquiring all data for histologic parameters and in vitro assays, the Student *t* test was applied to determine statistical significance. A *P* value of less than .05 was considered significant. Data analysis was performed by Microsoft Excel software (Microsoft, Redmond, WA).

Results

G-CSF Is Produced Within the Liver During OC-Mediated Regeneration and Acts as Both a Paracrine and Autocrine Factor on Hepatic OCs

Morphologic analysis of liver samples from animals subjected to BMTx/2AAF/PH (group C) confirmed the typical features of OC-mediated liver regeneration.[10] Specifically, in H&E-stained liver sections, oval-like cells, appearing as dark blue areas because of their large nuclei and scant cytoplasm, were seen surrounding the portal tracts after PH, and their number increased progressively, reaching a peak at day 11. These cells were positive for both OV6 and Ki67, indicating that they were proliferating OCs. Subsequently, the number and proliferation activity of OCs progressively decreased.

BM-derived cells were detected within the liver by their expression of DPPIV. Scattered patches of $DPPIV^+$, oval-like cells, and hepatocytes were detected. These patches ranged in size from single cells to small clusters. As for the magnitude of BM contribution to liver repopulation, in agreement with published data,[24] our study showed that the BM contribution to liver repopulation was a relatively rare event, resulting in a total contribution ($DPPIV^+$ OCs and hepatocytes within the recipients' livers) of 0.47% ± 0.12% at day 11 and 0.68% ± 0.21% at day 28 after PH. At day 11, the majority of the $DPPIV^+$ cells had an oval-like morphology and were concentrated within the periportal $OV6^+$ areas, whereas at day 28 the majority of the $DPPIV^+$ cells were hepatocyte-like.

To assess whether G-CSF may act directly on OCs, we studied the expression of G-CSFR in liver samples. G-CSFR was not expressed in normal liver, whereas it was induced during OC-mediated liver regeneration. Immunofluorescence revealed that G-CSFR was expressed by ductular and periductular cells after OC activation, colocalizing with the OC marker AFP (Figure 2*A*–*C*). G-CSF expression was detected in periportal cells and colocalized with G-CSFR within the OC population (Figure 2*D*–*F*). Confocal microscopy was used to confirm these findings on representative sections (Figure 2*G*–*I*). Western blot analysis revealed that G-CSFR was not produced by normal liver, whereas its expression was induced after OC activation. G-CSF production also was increased after 2AAF/PH, peaking between days 5 and 7 after surgery (Figure 3*A*). Finally, hepatic expression of G-CSFR mRNA was established through RT-PCR, performed on freshly isolated OCs, cultured OCs, and normal liver tissue (Figure 3*B*).

Hepatotrophic Effects of G-CSF Administration During OC-Mediated Liver Regeneration

To assess the effects of exogenous G-CSF during OC-mediated liver regeneration, BMTx/2AAF/PH pre-treated rats were subjected to G-CSF administration after surgery. We analyzed several parameters, such as the proliferation index ($Ki67^+$) and the magnitude of the OC reaction ($OV6^+$) in G-CSF–treated rats vs untreated rats. We compared 2 different molecular forms of G-CSF: recombinant methionyl human G-CSF (group B) and its pegylated counterpart (Peg–G-CSF, group A). An augmented OC reaction, relative to

controls, was observed in both of the G-CSF–treated groups (Figures 4 and 5). Particularly at day 11 after 2AAF/PH, the magnitude of the OC reaction was increased up to 5 times in animals treated with Peg–G-CSF and up to 2 times after G-CSF injection, as compared with controls ($P < 0.05$) (Figure 4*A*–*C*). At day 28, when only a few OCs still were present in 2AAF/PH controls, the number of liver OCs remained significantly higher in G-CSF– and Peg–G-CSF–treated rats (up to a 5- and 9-fold increase, respectively; $P < .05$). The highest OC response was measured in rats injected with Peg–G-CSF, although this increase was not statistically significant when compared with nonpegylated–G-CSF–treated animals (Figure 5*A*). The proliferation index also was increased significantly in animals treated with G-CSF or Peg–G-CSF (data not shown).

In an effort to evaluate the degree of BM contribution to liver repopulation after G-CSF administration, we quantified the number of donor-derived cells ($DPPIV^+$) in all groups. In serial sections, $DPPIV^+$ cells were seen predominantly within clusters of OC ($OV6^+$) (Figure 4*D* and *E*). Double immunofluorescence for OV6 and CD26 (DPPIV) confirmed the epithelial nature of the donor-derived cells within the liver (Figure 4*F*–*K*). The number of $DPPIV^+$ liver cells was significantly higher after G-CSF treatment (Figure 5*B*). Indeed, the number of donor-derived BM cells engrafted into the livers of G-CSF– and Peg–G-CSF–treated animals was proportionally higher at each time point vs controls, reaching a 4-fold increase at day 11 in group B ($P < .05$). In animals treated with G-CSF and Peg–G-CSF the average number of $DPPIV^+$ liver cells at day 11 represented, respectively, 2.06% ± .15% and 1.58% ± .84% of the entire liver population. At day 28, $DPPIV^+$ liver cells represented, respectively, 4.16% ± .62% (G-CSF) and 4.23% ± .75% (Peg–G-CSF) of the whole liver cell population, an increase of up to 6-fold as compared with controls (group A vs C, $P < .05$).

Immunofluorescence confirmed the expression of G-CSF and G-CSFR within the OC population after treatment with exogenous G-CSF (Figure 6*A*–*C*). G-CSFR co-localized with AFP (Figure 6*D*–*F*), whereas only a few $G\text{-}CSFR^+$ cells were hematopoietic cells ($CD45^+$), thereby excluding the possibility of significant hematopoietic cell contamination (Figure 6*G*–*I*).

G-CSFR Is Expressed Largely by Thy-1$^+$ Sorted OCs and G-CSF Promotes Both Migration and Proliferation of Hepatic OCs In Vitro

OCs were isolated using the hematopoietic immunomarker Thy-1 in conjunction with magnetic cell sorting.[10,22] In our study, we obtained an average of 3.5×10^6 $Thy\text{-}1^+$ cells from each liver. To test the specificity of the sorting procedure, cytospin preparations of $Thy\text{-}1^+$ cells were stained for Thy-1, OV6, and CD45 (Figure 7*A*–*C*). Approximately 95.8% ± 2.3% of the cells were $Thy\text{-}1^+$, 86.2% ± 7.5% were $OV6^+$, and the degree of hematopoietic cell contamination was negligible (2.2% ± 1.3% $CD45^+$). Double-immunofluorescence staining for G-CSFR and the hematopoietic marker CD45 confirmed that numerous $Thy\text{-}1^+$ cells expressed G-CSFR (58.7% ± 5.3%), whereas the few $CD45^+$ cells that were present did not express G-CSFR (Figure 7*D*–*F*). A further demonstration of the ability of OC to express G-CSFR was obtained by double-immunofluorescence staining for G-CSFR and the OC marker OV6. Most of the sorted cells were $OV6^+$ (≈86%), and a majority of them co-expressed G-CSFR (≈59%) (Figures 8*A*–*C* and 9). Moreover, most of the Thy-1 sorted cells co-expressed G-CSF and its receptor (Figure 8*D*–*F*).

As previously stated, OCs are able to proliferate in response to certain liver injuries and actively migrate from the portal tract periphery into the lobular parenchyma. We investigated the potential role of G-CSF in both OC proliferation and motility. G-CSF, at a concentration of 100 ng/mL, was able to significantly stimulate OC proliferation as compared with negative controls ($P < .05$), whereas lower or higher doses had only a slight

effect on proliferation (Figure 10*A*). In the migration assay, when G-CSF was added to the lower chamber, OCs crossed the filter in a dose-dependent manner, reaching a peak in the presence of 100 ng/mL of G-CSF (>6-fold increase after 6 hours, $P < .0001$) (Figure 10*B*). Interestingly, higher doses of G-CSF (500 ng/mL) did not affect cell motility.

Discussion

In the present study we have shown that G-CSF contributes to liver regeneration, both by increasing the engraftment of BMCs into the liver, and by enhancing the endogenous OC reaction. G-CSF acts on hepatic OCs as both an autocrine and a paracrine factor, and it is able to stimulate OC proliferation and migration in vitro. The effects of G-CSF on OC motility and proliferation are dose-dependent, reaching peak efficacy at 100 ng/mL. We speculate that the lack of an effect with higher doses may be owing to positive-feedback signals trigged by saturation of the G-CSFR.

G-CSF is a cytokine synthesized by a variety of cell types, and it is known to be involved in the proliferation and differentiation of granulocytes and their precursors, as well as in mediating hematopoietic stem cell mobilization to peripheral blood.[12,13] Recent studies have indicated that G-CSF may be effective in mobilizing cells that contribute to liver repair. BMCs mobilized by G-CSF contributed to hepatic regeneration after acute and chronic damage induced by CCl_4 in a murine model.16 G-CSF administration, during CCl_4 recurrent liver injury, significantly increased the number of BM-derived hepatocytes.[17] G-CSF stimulated peripheral blood BMCs to give rise to albumin-producing hepatocytes after infusion into analbuminemic rats.[18] Finally, G-CSF administration was able to induce BMC mobilization in cirrhotic patients, and a clinical improvement was registered in about 50% of treated individuals.[25] However, it remains unclear if G-CSF acts mainly by recruiting BMCs, or if it acts locally to facilitate the endogenous hepatic restoration program. Indeed, in the previously cited studies, G-CSF administration significantly accelerated the regeneration processes. Nevertheless, the level of BMC engraftment remained rather low, suggesting that G-CSF exerts a predominantly hepatotrophic effect, promoting the endogenous repair program. This hypothesis is supported by other reports showing the efficacy of G-CSF administration before hepatic damage. Theocharis et al[26] first reported that pretreatment with G-CSF significantly promotes DNA synthesis after liver injury, and recently showed that G-CSF improves survival rate in a rat model of fulminant hepatic failure.[27] They speculated that G-CSF facilitates hepatic proliferation by enhancing the expression of growth factors and proto-oncogenes, but the physiologic and pharmacologic mechanisms of this facilitation were not elucidated.[26,27] In the present study, we showed that G-CSF acts on OCs, the putative liver stem cells, affecting their proliferation and motility. Our results expand the knowledge regarding the spectrum of actions of G-CSF on adult stem cells. In fact, it has been shown that G-CSF acts not only on myeloid precursors, but also on neural and muscle stem/progenitor cells. In particular, recent reports have shown that G-CSF and its receptor are widely present in neurons and adult neural stem cells. This expression is induced by ischemia, and both counteracts neuronal degeneration and contributes to long-term plasticity after damage.[28,29] Similarly, G-CSF administration after myocardial infarction in mice induces G-CSFR expression in cardiomyocytes and results in the prevention of cardiac remodeling.[30]

Regarding the BMC contribution to liver regeneration, our study shows that the number of BM-derived hepatic cells in G-CSF–treated animals was increased up to 6-fold, as compared with the controls. Peg–G-CSF seemed to be more effective than the nonpegylated molecule, probably owing to an increased serum half-life, even though the difference was not statistically significant (group A vs B, $P > .05$). However, the level of BMC contribution in our experiments did not reach those of other models. Several factors appear to affect the

contribution of BMCs to liver repair. These include the nature, severity, and persistence of injury, as well as the dosage and timing of drug administration. A recent review of several published studies reported a frequency of less than 0.05% of BM-derived hepatocyte-like cells, when no selective pressures designed to increase the yield of BM contribution were used. When hepatocyte proliferation was inhibited, only half of the analyzed reports showed yields greater than 1.5%.[24] Although these levels of BM contribution would seem to preclude BMC as an effective tool for enhancing organ regeneration, the few BMCs that do engraft may play an important role in modulating the endogenous repair mechanisms. We showed that human cord blood hematopoietic stem cell administration represents a rescue therapy after liver injury in rats and nonobese diabetic/severe combined immunodeficiency mice.[8,9] The engrafted BMCs were able to facilitate hepatic repair, partly by conversion into liver cells, and partly by modulating the liver microenvironment. As for the effects of G-CSF on the hepatic regeneration, it has been suggested that G-CSF may act as a "yet unrecognized hepatocyte-growth factor inducer."[16] The existence of hepatocyte growth factors has been reported extensively, and their interactions and synergies are important elements in controlling the regenerative processes. Some of these molecules also are able to affect OC activation, but most of the specific liver stem cell–stimulating factors remain unknown. In the present study we have shown that G-CSF per se acts as a growth factor and a mobilizing agent for hepatic OCs. These results may help to elucidate the physiologic and pharmacologic mechanisms underlying the effects of G-CSF observed in previously reported studies. Furthermore, G-CSF might represent a critical factor for multiple lineages of tissue-committed stem cells, given that it exerts direct trophic effects on adult stem cells within the BM, muscle, nerve, and, as we now have shown, the liver.

As for the cellular mechanisms underlying the BMC conversion into hepatic cells, it has been observed that cell fusion may explain some of the presumed plasticity of BMCs seen in specific models of liver regeneration.[31] However, other convincing data indicate that liver repopulation is possible without fusion.[22] We believe that fusion may or may not play a prominent role in the plasticity of stem cells, depending on the model of injury and the host phenotype.[31] In our model, hepatocyte proliferation was inhibited at the time of G-CSF administration, and the direct BM contribution to liver regeneration remained a relatively rare phenomenon, whereas the local effect of the drug on the endogenous OC population seems the most likely mechanism to explain our findings. The current study does not focus on the ultimate origin of the BMCs that are participating in liver regeneration. If a portion of these cells do arise from a fusion event, but maintain functionality, they still are relevant therapeutically. Given the extent of endogenous OC participation as compared with BMCs, the action of G-CSF on endogenous liver cells is likely to have a greater therapeutic impact.

In conclusion, with the present study we have shown that G-CSF exerts multiple beneficial effects on hepatic repair programs, both by increasing the engraftment of BMCs into the liver, and by enhancing the endogenous OC reaction. Our results confirm the previously reported data on G-CSF mobilization of liver-committed BMCs, and further highlight the complexity of the mechanisms involved in the activation and trafficking of liver stem cells and their derivatives. G-CSF treatment is an appealing potential therapy for improving liver regeneration because it offers both ease of treatment and versatility. The present study provides the conceptual basis for the development of therapeutic strategies aimed at stimulating the proliferation, mobilization, and targeting of OCs to enhance recovery from hepatic injury.

Acknowledgments

Supported by grants PF-05-165-01 (T.D.S.) from the American Cancer Society and by grants 2R01DK058614-05 and R01DK065096 (B.E.P.) from the National Institutes of Health. A.C.P. also received support by the "*Pio*

Sodalizio dei Piceni" during her research. B.E.P. owns stock in ReGenMed and may receive royalties from license agreements from ReGenMed and as such may benefit financially as a result of the outcomes of research or work reported in this publication.

The authors are deeply appreciative to Amgen Inc. (Thousand Oaks, CA) for kindly providing the granulocyte–colony stimulating factor used in these studies. The authors also would like to thank Mr Andrea Primadei for technical support in the presentation of the data.

Abbreviations used in this paper

2AAF	2-acetylaminofluorene
AFP	α-fetoprotein
BMC	bone marrow cell
BMTx	bone marrow transplantation
DPPIV$^-$	dipeptidyl-peptidase-IV deficient
G-CSF	granulocyte–colony stimulating factor
G-CSFR	granulocyte–colony stimulating factor receptor
IMDM	Iscove's modified Dulbecco's medium
OC	oval cell
PCR	polymerase chain reaction
PH	partial hepatectomy
RT	reverse transcription

References

1. Shackel NA, Rockey DC. Stem cells and liver disease: promise laced with confusion and intrigue. Gastroenterology. 2004; 127:346–348. [PubMed: 15236208]
2. Lowes KN, Croager EJ, Olynyk JK, Abraham LJ, Yeoh GC. Oval cell-mediated liver regeneration: role of cytokines and growth factors. J Gastroenterol Hepatol. 2003; 18:4–12. [PubMed: 12519217]
3. Libbrecht L, Desmet V, Van Damme B, Roskams T. Deep intralobular extension of human hepatic progenitor cells correlates with parenchymal inflammation in chronic viral hepatitis: can progenitor cells migrate? J Pathol. 2000; 192:373–378. [PubMed: 11054721]
4. Crosbie OM, Reynolds M, McEntee G, Traynor O, Hegarty JE, O'Farrelly C. In vitro evidence for the presence of hematopoietic stem cells in the adult human liver. Hepatology. 1999; 29:1193–1198. [PubMed: 10094964]
5. Petersen BE, Bowen WC, Patrene KD, Mars WM, Sullivan AK, Murase N, Boggs SS, Greenberger JS, Goff JP. Bone marrow as a potential source of hepatic oval cells. Science. 1999; 284:1168–1170. [PubMed: 10325227]
6. Alison MR, Poulsom R, Jeffery R, Dhillon AP, Quaglia A, Jacob J, Novelli M, Prentice G, Williamson J, Wright NA. Hepatocytes from non-hepatic adult stem cells. Nature. 2000; 406:257. [PubMed: 10917519]
7. Theise ND, Nimmakayalu M, Gardner R, Illei PB, Morgan G, Teperman L, Henegariu O, Krause DS. Liver from bone marrow in humans. Hepatology. 2000; 32:11–16. [PubMed: 10869283]
8. Piscaglia AC, Di Campli C, Zocco MA, Di Gioacchino G, Novi M, Rutella S, Bonanno G, Monego G, Vecchio FM, Michetti F, Mancuso S, Leone G, Gasbarrini G, Pola P, Gasbarrini A. Human cordonal stem cell intraperitoneal injection can represent a rescue therapy after an acute hepatic damage in immunocompetent rats. Transplant Proc. 2005; 37:2711–2714. [PubMed: 16182791]
9. Piscaglia AC, Zocco MA, Di Campli C, Sparano L, Rutella S, Monego G, Bonanno G, Michetti F, Mancuso S, Pola P, Leone G, Gasbarrini G, Gasbarrini A. How does human stem cell therapy

influence gene expression after liver injury? Microarray evaluation on a rat model. Dig Liver Dis. 2005; 37:952–963. [PubMed: 16214431]

10. Petersen BE, Goff JP, Greenberger JS, Michalopoulos GK. Hepatic oval cells express the hematopoietic stem cell marker Thy-1 in the rat. Hepatology. 1998; 27:433–445. [PubMed: 9462642]
11. Petersen BE, Grossbard B, Hatch H, Pi L, Deng J, Scott EW. Mouse A6-positive hepatic oval cells also express several hematopoietic stem cell markers. Hepatology. 2003; 37:632–640. [PubMed: 12601361]
12. Szumilas P, Barcew K, Baskiewicz-Masiuk M, Wiszniewska B, Ratajczak MZ, Machalinski B. Effect of stem cell mobilization with cyclophosphamide plus granulocyte colony-stimulating factor on morphology of haematopoietic organs in mice. Cell Prolif. 2005; 38:47–61. [PubMed: 15679866]
13. Thomas J, Liu F, Link DC. Mechanisms of mobilization of hematopoietic progenitors with granulocyte colony-stimulating factor. Curr Opin Hematol. 2002; 9:183–189. [PubMed: 11953662]
14. Imamura R, Miyamoto T, Yoshimoto G, Kamezaki K, Ishikawa F, Henzan H, Kato K, Takase K, Numata A, Nagafuji K, Okamura T, Sata M, Harada M, Inaba S. Mobilization of human lymphoid progenitors after treatment with granulocyte colony-stimulating factor. J Immunol. 2005; 175:2647–2654. [PubMed: 16081841]
15. Ratajczak MZ, Kucia M, Reca R, Majka M, Janowska-Wieczorek A, Ratajczak J. Stem cell plasticity revisited: CXCR4-positive cells expressing mRNA for early muscle, liver and neural cells hide out in the bone marrow. Leukemia. 2004; 18:29–40. [PubMed: 14586476]
16. Yannaki E, Athanasiou E, Xagorari A, Constantinou V, Batsis I, Kaloyannidis P, Proya E, Anagnostopoulos A, Fassas A. G-CSF-primed hematopoietic stem cells or G-CSF per se accelerate recovery and improve survival after liver injury, predominantly by promoting endogenous repair programs. Exp Hematol. 2005; 33:108–119. [PubMed: 15661404]
17. Quintana-Bustamante O, Alvarez-Barrientos A, Kofman AV, Fabregat I, Bueren JA, Theise ND, Segovia JC. Hematopoietic mobilization in mice increases the presence of bone marrow-derived hepatocytes via in vivo cell fusion. Hepatology. 2006; 43:108–116. [PubMed: 16374873]
18. Huiling X, Inagaki M, Arikura J, Ozaki A, Onodera K, Ogawa K, Kasai S. Hepatocytes derived from peripheral blood stem cells of granulocyte-colony stimulating factor treated F344 rats in analbuminemic rat livers. J Surg Res. 2004; 122:75–82. [PubMed: 15522318]
19. Petersen BE, Zajac VF, Michalopoulos GK. Hepatic oval cell activation in response to injury following chemically induced periportal or pericentral damage in rats. Hepatology. 1998; 27:1030–1038. [PubMed: 9537443]
20. Alison MR, Golding M, Sarraf CE, Edwards RJ, Lalani EN. Liver damage in the rat induces hepatocyte stem cells from biliary epithelial cells. Gastroenterology. 1996; 110:1182–1190. [PubMed: 8613008]
21. Higgins GM, Anderson RM. Experimental pathology of the liver. I. Restoration of the liver of the white rat following partial surgical removal. Arch Pathol. 1931; 12:186–202.
22. Oh SE, Witek RP, Bae SH, Zheng D, Jung Y, Piscaglia AC, Petersen BE. Bone-marrow derived hepatic oval cells differentiate into hepatocytes in 2-acetylaminofluorene/partial hepatectomy-induced liver regeneration. Gastroenterology. 2007; 132:1077–1087. [PubMed: 17383429]
23. Jung Y, Oh SH, Zheng D, Shupe TD, Witek RP, Petersen BE. A potential role of somatostatin and its receptor SSTR4 in the migration of hepatic oval cells. Lab Invest. 2006; 86:477–489. [PubMed: 16534498]
24. Thorgeirsson SS, Grisham JW. Hematopoietic cells as hepatocyte stem cells: a critical review of the evidence. Hepatology. 2006; 43:2–8. [PubMed: 16374844]
25. Gaia S, Smedile A, Omede P, Olivero A, Sanavio F, Balzola F, Ottobrelli A, Abate ML, Marzano A, Rizzetto M, Tarella C. Feasibility and safety of G-CSF administration to induce bone marrow-derived cells mobilization in patients with end stage liver disease. J Hepatol. 2006; 45:13–19. [PubMed: 16635534]

26. Theocharis SE, Margeli AP, Goutas ND, Horti MG, Karkantaris CS, Kittas CN. Granulocyte colony-stimulating factor administration reverses cadmium-associated inhibition of hepatocyte regeneration. Eur J Gastroenterol Hepatol. 1996; 8:805–809. [PubMed: 8864679]

27. Theocharis SE, Papadimitriou LJ, Retsou ZP, Margeli AP, Ninos SS, Papadimitriou JD. Granulocyte-colony stimulating factor administration ameliorates liver regeneration in animal model of fulminant hepatic failure and encephalopathy. Dig Dis Sci. 2003; 48:1797–1803. [PubMed: 14561004]

28. Schabitz WR, Kollmar R, Schwaninger M, Juettler E, Bardutzky J, Scholzke MN, Sommer C, Schwab S. Neuroprotective effect of granulocyte colony-stimulating factor after focal cerebral ischemia. Stroke. 2003; 34:745–751. [PubMed: 12624302]

29. Schneider A, Kruger C, Steigleder T, Weber D, Pitzer C, Laage R, Aronowski J, Maurer MH, Gassler N, Mier W, Hasselblatt M, Kollmar R, Schwab S, Sommer C, Bach A, Kuhn HG, Schabitz WR. The hematopoietic factor G-CSF is a neuronal ligand that counteracts programmed cell death and drives neurogenesis. J Clin Invest. 2005; 115:2083–2098. [PubMed: 16007267]

30. Harada M, Qin Y, Takano H, Minamino T, Zou Y, Toko H, Ohtsuka M, Matsuura K, Sano M, Nishi J, Iwanaga K, Akazawa H, Kunieda T, Zhu W, Hasegawa H, Kunisada K, Nagai T, Nakaya H, Yamauchi-Takihara K, Komuro I. G-CSF prevents cardiac remodeling after myocardial infarction by activating the Jak-Stat pathway in cardiomyocytes. Nat Med. 2005; 11:305–311. [PubMed: 15723072]

31. Piscaglia AC, Shupe T, Gasbarrini A, Petersen BE. Microarray RNA/DNA in different stem cell lines. Curr Pharmaceut Biotechnol. 2007; 8:167–175.

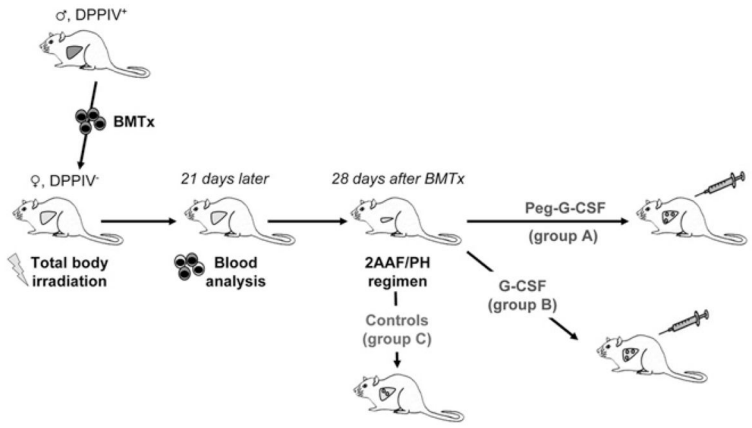

Figure 1.

Experimental design. DPPIV-female rats were exposed to total body γ-irradiation, before BMTx. BMCs were isolated from wild-type male rats and transplanted into recipient rats. Three weeks later, donor contribution to BM reconstitution was assessed. Four weeks after BMTx, chimeric animals were implanted with a 2AAF pellet, and 7 days later rats underwent PH. After surgery, animals were administered Peg–G-CSF (group A), or nonpegylated G-CSF (group B). Control rats did not receive any further treatment (group C).

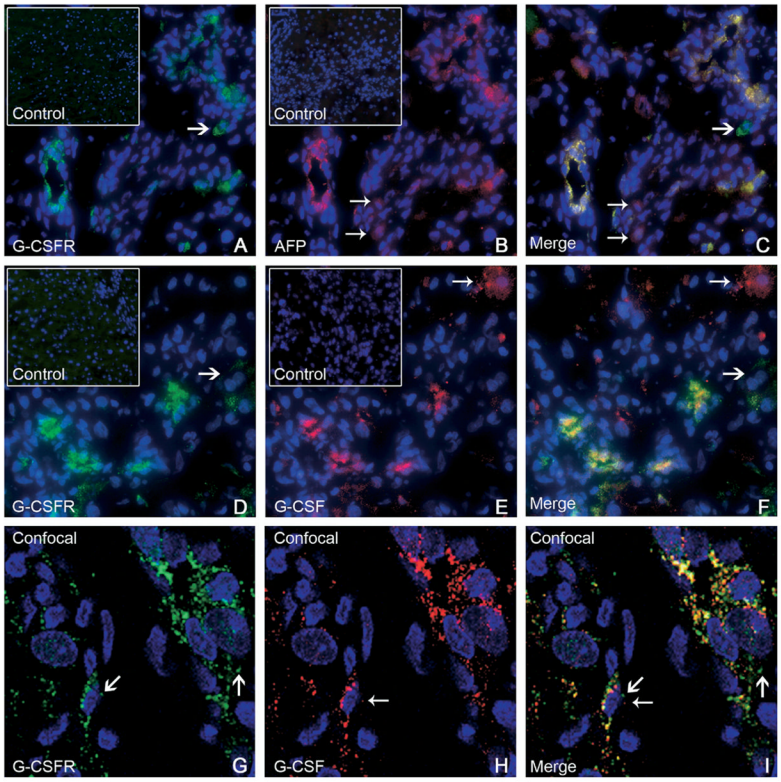

Figure 2.

(*A–C*) Double-immunofluorescence staining of livers from group C (11 days after 2AAF/PH) showed expression of (*A*) G-CSFR (*green*), (*B*) AFP (*red*), and (*C*) co-expression (*yellow*) by many periportal cells. A few cells expressed AFP alone (*small arrows*, 2*B* and 2*C*), or G-CSFR alone (*large arrows*, 2*A* and 2*C*). The inserts in *A* and *B* represent isotype controls for G-CSFR and AFP, respectively. Cell nuclei were stained with DAPI (*blue*). Original magnification, 40× objective. (*D–F*) Double-immunofluorescence staining of livers from group C (11 days after 2AAF/PH) detected cells expressing (*D*) G-CSFR (*green*), (*E*) G-CSF (*red*), and (*F*) co-expression (*yellow*) in many periportal cells. A few cells expressed G-CSFR alone (*large arrows*, 2*D* and 2*F*) or G-CSF alone (*small arrows*, 2*E* and 2*F*). The inserts in *D* and *E* represent isotype controls for G-CSFR and G-CSF, respectively. Cell nuclei were stained with DAPI (*blue*). Original magnification, 40× objective. (*G–I*) Confocal microscopy was used on representative sections from the same animals (group C). Immunofluorescence for (*G*) G-CSFR (*green*) and (*H*) G-CSF (*red*) shows (*I*) co-expression (merge) within many periportal cells. The presence of dual markers (*yellow*) is evident in most cells shown. Both G-CSFR and G-CSF also were seen as distinct colors in separate cellular domains, denoting differential distribution within the cell (*large arrows* and *small arrows*, respectively). Cell nuclei were stained with DAPI (*blue*). Original magnification, 63× objective.

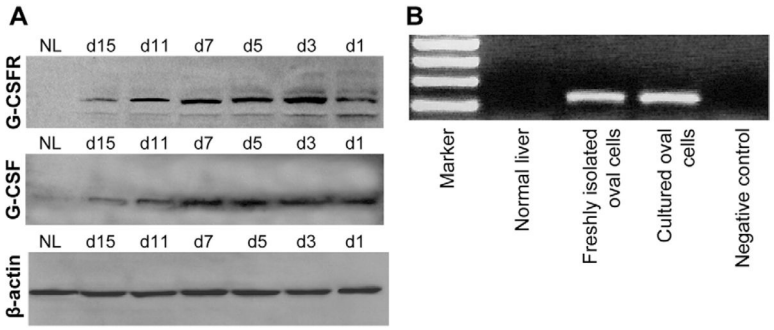

Figure 3.

(*A*) Western blot analysis of liver homogenates confirmed the expression of both G-CSF and G-CSFR after 2AAF/PH in rats (at days 1, 3, 5, 7, 11, and 15 after surgery) vs normal liver (NL). G-CSFR was not produced by NL, whereas its expression was induced after OC activation, with a peak at days 3–7 after PH. G-CSF production also was increased after 2AAF/PH, peaking at days 5–7 after PH. (*B*) RT-PCR amplification of G-CSFR mRNA in normal liver, freshly isolated OCs, and cultured OCs provide further proof of the expression of G-CSFR by hepatic OCs.

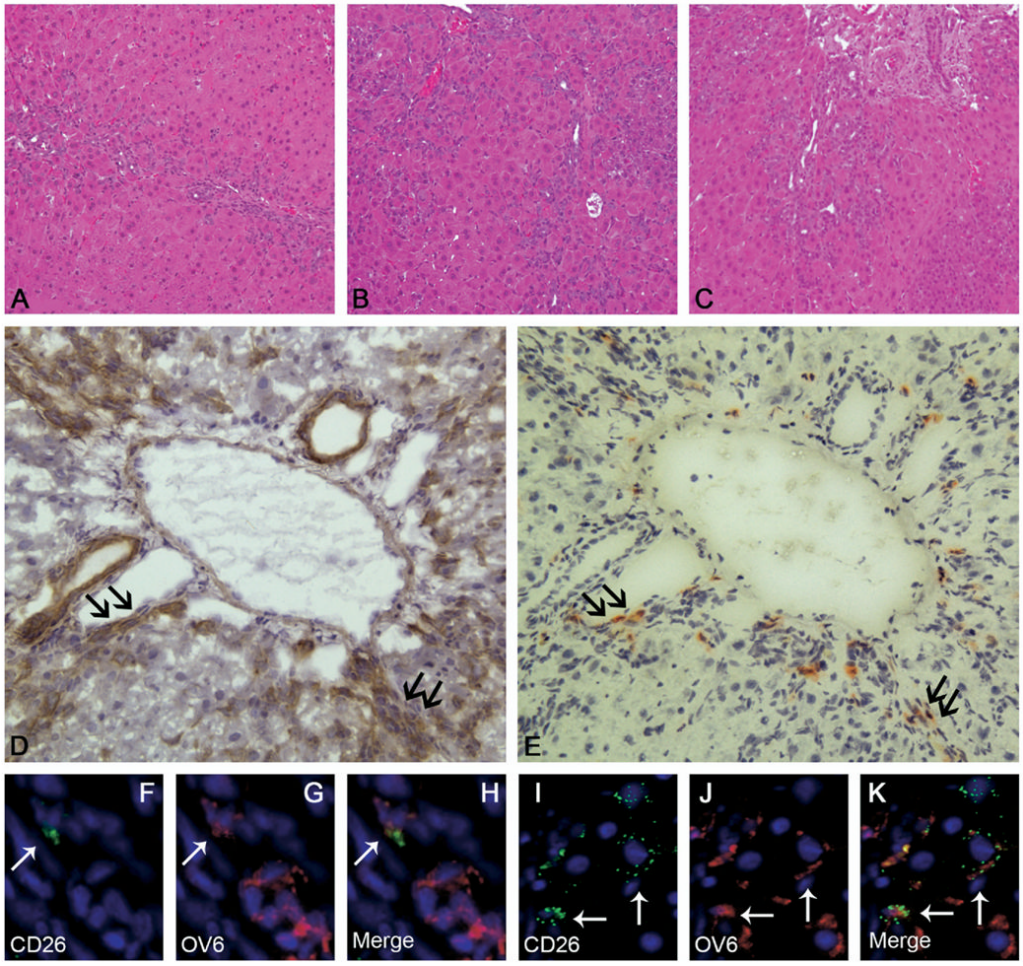

Figure 4.

H&E staining of liver sections 11 days after 2AAF/PH in (*A*) control animals (group C), (*B*) after G-CSF treatment (group B), and (*C*) after Peg–G-CSF administration (group A). At the peak of the OC reaction, the number of OCs was significantly higher in animals treated with G-CSF or Peg–G-CSF as compared with controls. Original magnification, 10× objective. (*D* and *E*) Representative serial sections stained for OV6 and DPPIV in the liver of a BMTx/2AAF/PH rat treated with exogenous G-CSF (group A). The expression of DPPIV represents a specific marker of BM donor–derived cells. (*E*) Right panel shows expression of DPPIV on many small, periportal cells (*red–orange*). (*D*) The corresponding serial section depicted in the left panel shows that many of the $DPPIV^+$ cells also express the OC marker OV6 (*brown*), and therefore may be considered BM-derived OCs. Black arrows indicate the same cells on each figure. Original magnification, 20× objective. (*F–K*) Double-immunofluorescence staining of liver from group A (11 days after 2AAF/PH) detected cells expressing (anti-DPPIV, 4*F* and 4*I*, *green*) CD26, (4*G* and 4*J*, red) OV6, and (4*H* and 4*K*, *yellow*) co-expression in many periportal cells (⇐). Cell nuclei were stained with DAPI (*blue*). Original magnification, 40× objective.

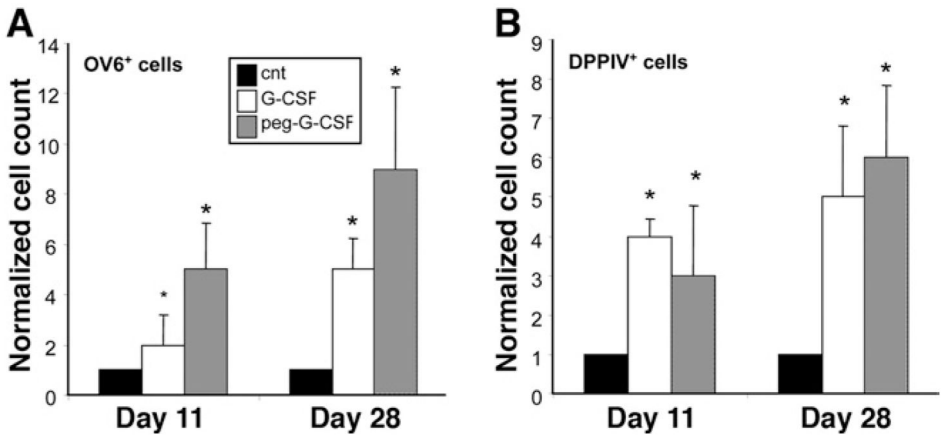

Figure 5.

(*A*) Average $OV6^+$ cells/field in livers of animals treated with either pegylated or nonpegylated G-CSF at 11 and 28 days after 2AAF/PH, as compared with 2AAF/PH alone (CNT). (*B*) Average $DPPIV^+$ cells/field in livers of animals treated with either pegylated or nonpegylated G-CSF at 11 and 28 days after 2AAF/PH, as compared with 2AAF/PH alone (cnt). Data represent the mean value + SD of cell counts, normalized with respect to control. $*P < .05$. At day 11 after 2AAF/PH, the magnitude of the OC reaction was increased up to 5 times in animals treated with Peg–G-CSF as compared with controls. At day 28, when only a few OCs still were present in 2AAF/PH controls, the number of liver OCs remained significantly higher in G-CSF– and Peg–G-CSF–treated rats (up to 9-fold increase). Similarly, the number of donor-derived BMCs engrafted into the livers of G-CSF– and Peg–G-CSF–treated animals was proportionally higher at each time point, reaching a 4-fold increase at day 11 and a 6-fold increase at day 28 after PH.

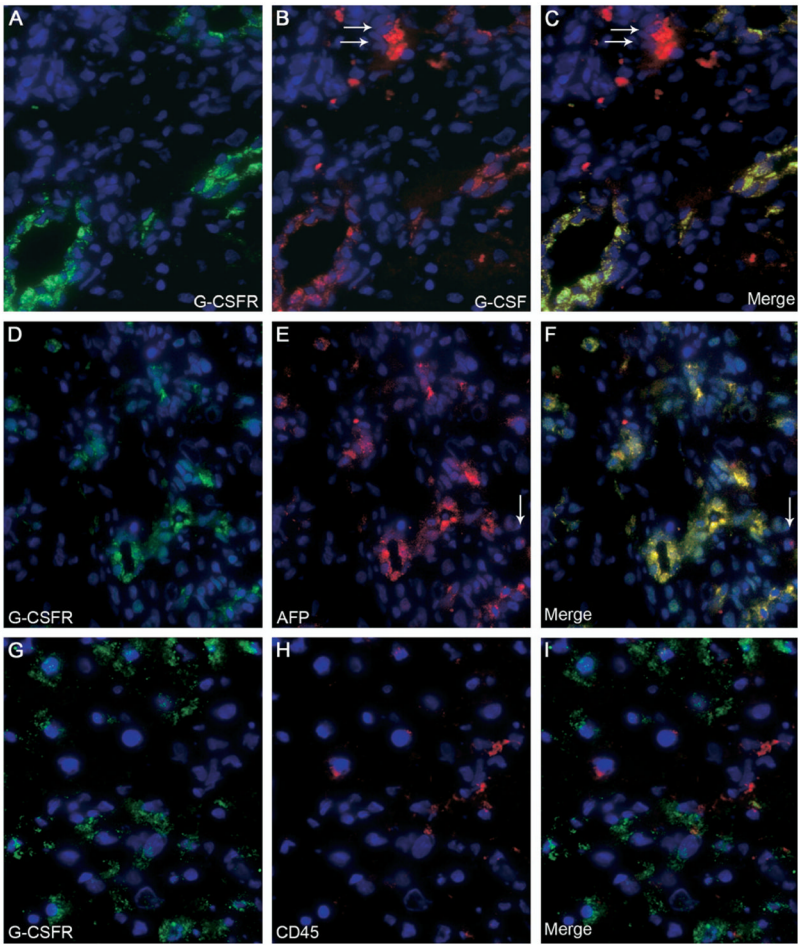

Figure 6.

(*A*–*C*) Double-immunofluorescence staining on liver section 11 days after 2AAF/PH/G-CSF treatment (group B) detected (*A*) G-CSFR (*green*), (*B*) G-CSF (*red*), and (*C*) co-expression (*yellow*) by many periportal cells. A few cells expressed G-CSF alone (⇐, 6*B* and 6*C*). (*D*–*F*) Double-immunofluorescence staining of liver 11 days after 2AAF/PH/G-CSF treatment (group B) showed expression of (*D*) G-CSFR (*green*), (*E*) AFP (*red*), and (*F*) co-expression (*yellow*) by many periportal cells. A few cells expressed AFP alone (⇐, 6*E* and 6*F*). (*G*–*I*) Double-immunofluorescence staining of liver 11 days after 2AAF/PH/G-CSF treatment (group B) detected (*G*) G-CSFR (*green*) and (*H*) CD45 (*red*). (*I*) The merge of panels *G* and *H* showed that G-CSFR$^+$ cells were mostly CD45$^-$, thereby excluding the possibility of significant hematopoietic cell contamination. Cell nuclei were stained with DAPI (*blue*). Original magnification, 40× objective.

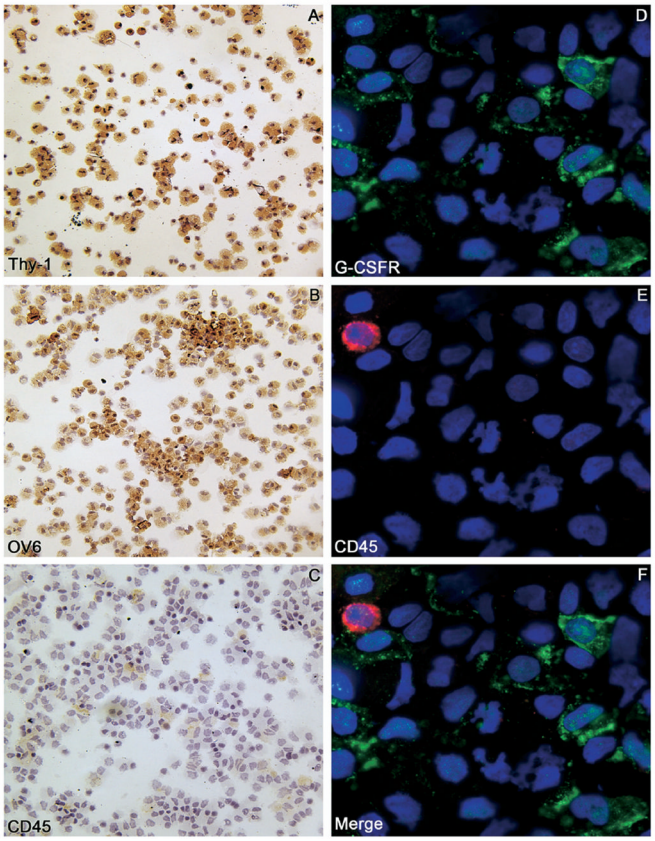

Figure 7.

(*A*–*C*) Thy-1$^+$ sorted cell cytospins stained for (*A*) Thy-1, (*B*) OV6, and (*C*) CD45. Most of the sorted cells were OV6$^+$ and Thy-1$^+$, whereas a very few hematopoietic cells (CD45$^+$) were observed. (*D*–*F*) Double-immunofluorescence staining of Thy-1$^+$ sorted cell cytospins show (*D*) G-CSFR (*green*) and (*E*) the hematopoietic marker CD45 (*red*). Numerous Thy-1$^+$ cells expressed G-CSFR (~59%), whereas the degree of hematopoietic cell contamination was negligible. (*F*) The merge of panels *D* and *E* showed that the few CD45$^+$ cells were G-CSFR$^-$. Cell nuclei were stained with DAPI (*blue*). Original magnification, 100× objective.

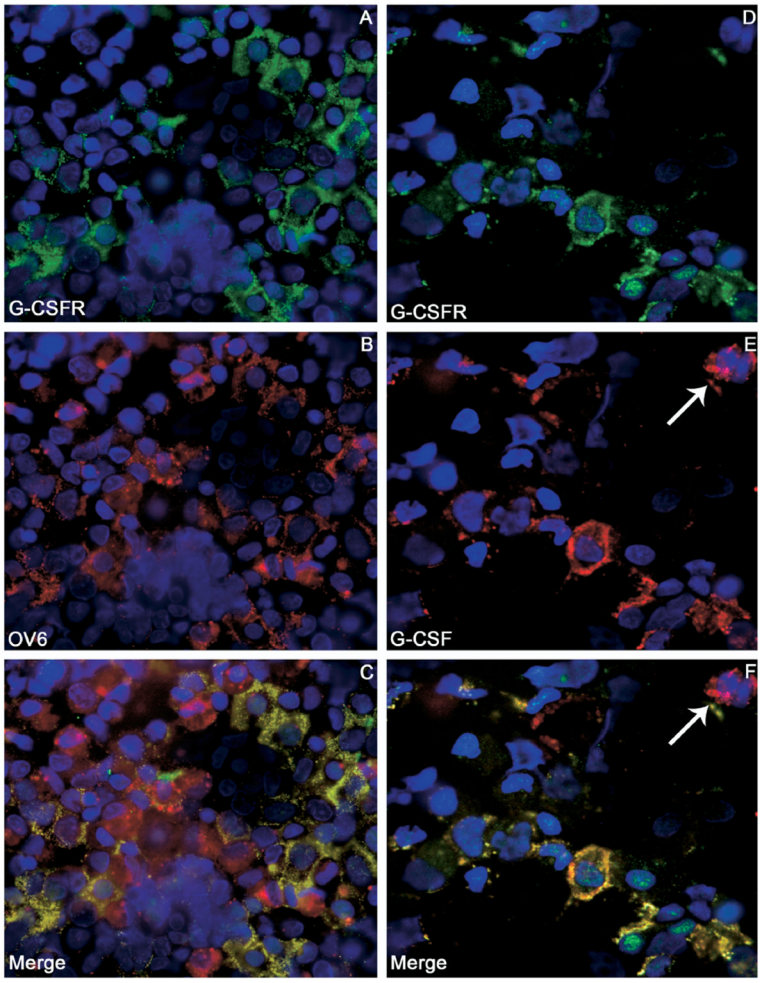

Figure 8.

(*A*–*C*) Double-immunofluorescence staining of Thy-1$^+$ sorted cell cytospins showed the expression of (*A*) G-CSFR (*green*) and (*B*) the OC marker OV6 (*red*). Most of the sorted cells were OV6 positive (~86%), and a majority also expressed G-CSFR (~59%). (*C*) The merge of panels *A* and *B* showed that all of the G-CSFR$^+$ cells also expressed OV6. (*D*–*F*) Double-immunofluorescence staining of Thy-1$^+$ sorted cell cytospins stained for (*D*) G-CSFR (*green*) and (*E*) G-CSF (*red*). (*F*) The merge of panels *D* and *E* shows that most of the Thy-1 sorted cells co-expressed G-CSF and G-CSFR (*yellow*), whereas a few were only G-CSF$^+$ (⇐). Cell nuclei were stained with DAPI (*blue*). Original magnification, 100×.

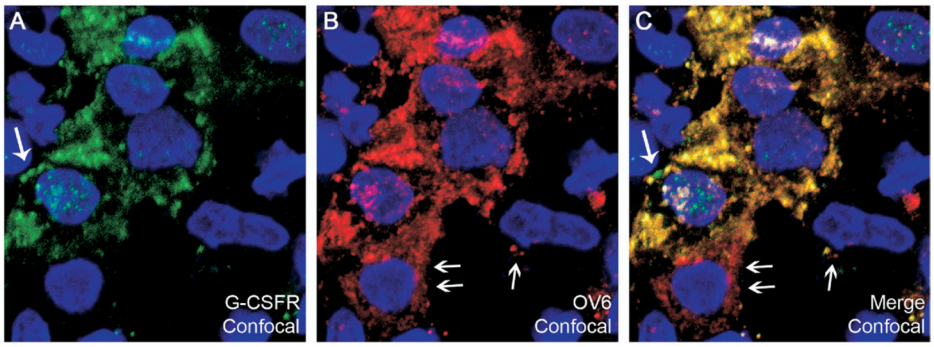

Figure 9.

(*A*–*C*) Confocal microscopy of double-immunofluorescence staining of Thy-1^{+} sorted cell cytospins for (*A*) G-CSFR (*green*), (*B*) OV6 (*red*), and (*C*) co-expression (*yellow*). Note that the distribution of these proteins within the cell is not identical (*large* and *small arrows*, respectively). Cell nuclei were stained with DAPI (*blue*). Confocal magnification, 252× (63× objective combined with 4× digital zoom).

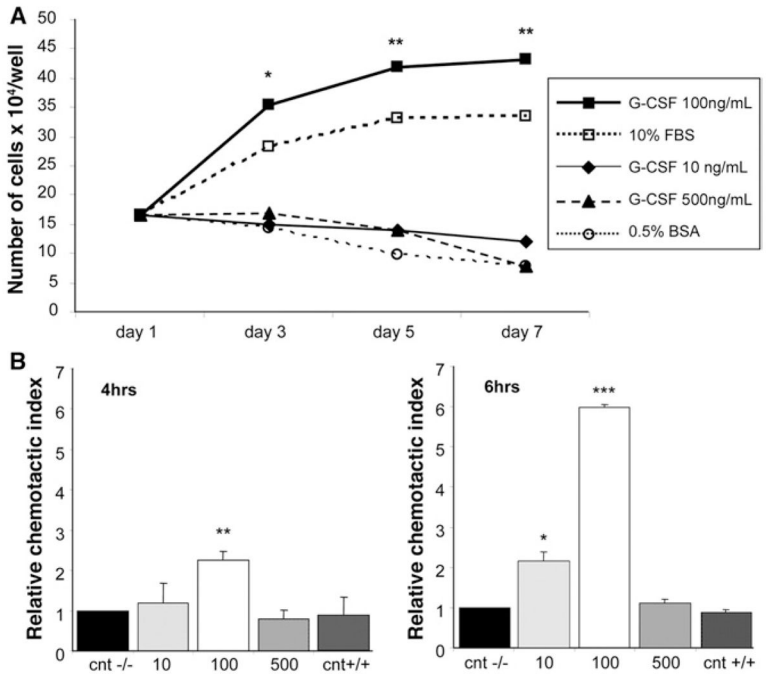

Figure 10.

(*A*) Effects of G-CSF on OC proliferation. OCs were incubated in IMDM medium supplemented with 10% fetal bovine serum (□), or serum-free IMDM medium containing 0.5% bovine serum albumin with G-CSF at 10 ng/mL (◆), 100 ng/mL (■), 500 ng/mL (▲), or without G-CSF (○, negative control) for the indicated times. Differences were statistically significant when comparing 100 ng/mL G-CSF vs negative controls. **P* < 0.05, ***P* < .005. (*B*) Effect of G-CSF on OC migration in transwells. OCs were seeded in the top chamber with 10, 100, or 500 ng/mL G-CSF placed in the bottom chamber, or 100 ng/mL of G-CSF placed in both chambers (CNT+/+, chemokinetic control). Migration controls were used with no G-CSF in either chamber (cnt−/−). Data represent the mean value + SD of 3 independent experiments, normalized with respect to control migration (relative chemotactic index; **P* < .05, ***P* < .01, ****P* < .0001). When G-CSF was added to the lower chamber, OCs crossed the filter in a dose-dependent manner, reaching a peak in the presence of 100 ng/mL of G-CSF (>6-fold increase after 6 hours).